Ultrasonics Sonochemistry 90 (2022) 106183

Contents lists available at ScienceDirect

Ultrasonics Sonochemistry

journal homepage: www.elsevier.com/locate/ultson

Chemoenzymatic surface decoration of Nisin-shelled nanoemulsions: Novel targeted drug-nanocarriers for cancer applications

Rania A. Hashad [a,b,f], Ritu Singla [c], Sukhvir Kaur Bhangu [c], Edwina Jap [a], Haiyan Zhu [c,d], Anton Y. Peleg [e], Luke Blakeway [e], Christoph E. Hagemeyer [b], Francesca Cavalieri [d], Muthupandian Ashokkumar [c], Karen Alt [a,*]

[a] NanoTheranostics Laboratory, Australian Center for Blood Diseases, Monash University, Melbourne, VIC 3004, Australia
[b] NanoBiotechnology Laboratory, Australian Center for Blood Diseases, Monash University, Melbourne, VIC 3004, Australia
[c] School of Chemistry, University of Melbourne, VIC 3010, Australia
[d] School of Science, RMIT University, Melbourne, VIC 3000, Australia
[e] Department of Infectious Diseases, The Alfred Hospital & Monash University, VIC 3004, Australia
[f] Department of Pharmaceutics and Industrial Pharmacy, Faculty of Pharmacy, AinShamsUniversity, Cairo, Egypt

ARTICLE INFO

Keywords:
Nanoemulsion
Ultrasonication
Nisin
Drug delivery

ABSTRACT

Nisin, a peptide used as a natural food preservative, is employed in this work for the development of a novel nanocarrier system. Stable and uniform nisin-shelled nanoemulsions (NSNE) with a diameter of 100 ± 20 nm were successfully prepared using 20 kHz flow-through ultrasonication technique. The NSNE showed limited toxicity, high bactericidal activity and high drug loading capacity (EE 65 % w/w). In addition, the nisin shell was exploited for the site-specific attachment of a recombinantly produced cancer targeting ligand ($\alpha HER2_{LPETG}$ IgG). Employing a unique two phases (bio-click) approach which involved both Sortase A mediated Azide Bio-conjugation (SMAB) and Strain Promoted Azide Alkyne Cycloaddition (SPAAC) reactions, targeted NSNE ($NSNE_{DOX}$-αHER2 IgG) were successfully assembled and loaded with the chemotherapeutic drug Doxorubicin (DOX). Finally, $NSNE_{DOX}$-αHER2 IgG showed cancer-specific binding and augmented cytotoxicity to HER2 expressing tumour cells.

1. Introduction

Development of novel therapeutic strategies is of paramount importance in translational biomedical research. Protein shelled nanoemulsions (PSNE) can offer a versatile platform for targeted drug delivery. While the protein in the shell provides a non-toxic, biocompatible, and biodegradable surface that is rich in functional groups for the attachment of targeting ligands [1–3], the nanoemulsion core acts as a drug carrier. PSNE as a targeted nano-delivery system, can significantly enhance therapeutic efficacy, avoid toxicity and minimize side effects [4], which is particularly important for drug delivery of chemotherapeutics. Here, we introduce a facile protocol for the preparation of novel protein shelled nanoemulsions for potential targeted cancer therapy.

Ultrasonic emulsification is a simple, fast, versatile, and green pathway for preparing PSNE [5]. In previous studies Zhou et al have shown that the active cavitation zone in the flow through horn is limited to the hole region [6]. Hence uniform nanoemulsions are typically obtained due to the confinement of the active cavitation zone in the hole region. This flow through ultrasonication technique is adopted in this study to produce monodisperse oil in water nanoemulsions stabilized by a protein coating.

Numerous proteins and peptides have been investigated as building blocks for engineering nanodrug delivery. These include human serum albumin, gelatin, gliadins, lipoproteins and ferritin [1]. Nisin is a cationic peptide produced by *Lactococcus lactis* that is widely used in the food industry as an antimicrobial preservative for inhibiting the growth of gram-positive bacteria and other pathogen [7], and may provide a natural, cheap, and readily available nanodrug delivery system that is yet to be explored. Over the past two decades, studies have shown the use of nisin for various biomedical applications beyond its bactericidal activity. Joo et al. explored the cytotoxic and antitumour properties of nisin A and discovered that it blocks head and neck squamous cell carcinoma tumourigenesis [8]. Moreover, Nakajima et. al discovered the

* Corresponding author.
E-mail address: karen.alt@monash.edu (K. Alt).

https://doi.org/10.1016/j.ultsonch.2022.106183
Received 3 March 2022; Received in revised form 4 August 2022; Accepted 5 August 2022
Available online 28 September 2022

excellent emulsifying power of this small amphiphilic cationic peptide [9]. Surface activity studies performed in the presence of soybean oil showed a significant emulsifying capacity of nisin at the concentration of 10 mg nisin/mL, as compared to β-casein and Tween 80. Nisin is therefore selected as the peptide of choice for the preparation of NSNE based on its biological and physicochemical properties. Specific to this work, the inherent anti-cancer activity of nisin can provide adjuvant therapeutic value to a chemotherapeutic drug payload. Doxorubicin was chosen as a model payload for this application.

The surface topography of NSNE is particularly important to create a docking platform for targeting ligands on their surface as illustrated in the schematic overview. Lysine, available in the structure of nisin, is one of the most commonly modified residues for protein modification and reacts spontaneously with *N*-hydroxysuccinimidyl (NHS) ester. When the free amine groups in the nisin shell are incubated with a bifunctional amine reactive linker (NHS-PEG-BCN), the nanocarrier surface becomes tethered with bicyclononyne (BCN) click handles. Depending on the surface modification, the resulting particles (NSNE-BCN) can spontaneously conjugate to a smart fluorescent click (SFC) probe, specially engineered by Ji et al to emit fluorescence only after biorthogonal click activation [10].

Bioorthogonal click chemistry is a highly specific and powerful chemical conjugation method inert to biological degradation [11]. Two major types of bioorthogonal click reactions are prevalent, namely copper (I)-catalysed azide-alkyne cycloaddition (CuAAC) and strain-promoted azide-alkyne cycloaddition (SPAAC) [12–13]. SPAAC reaction is the second component of a unique two-step 'bio-click' approach, well established by Hagemeyer et al. for nanomedicine applications [14–15], and employed hereby for site-specific modification and conjugation of a target ligand to NSNE surface.

Initially, Sortase A (SrtA), a transpeptidase enzyme naturally produced by *Staphylococcus aureus* [16] was expressed and purified in *E. Coli*. SrtA was then used to catalyze the bioconjugation of a click functionality (specifically an azide) to a genetically encoded targeting antibody carrying SrtA recognition motif (LPETG). The strained-alkyne click group (specifically BCN) is tethered to the nanoparticle surface. Therefore, SPAAC reaction drives the site-specific covalent attachment of the targeting ligand to NSNE surface. In contrast to traditional chemical non-specific conjugation strategies, this 'bio-click' chemoenzymatic conjugation avoids compromising the affinity of the antigen-binding site for the target [14].

Targeted NSNE provides a nano-sized platform for numerous biomedical applications. Specifically, for this study, an αHER2 IgG monoclonal antibody was used as the targeting ligand to investigate the anti-neoplastic activity of this novel nanosystem (NSNE). The human epidermal growth factor receptor 2 (HER2) is a member of the quartet human EGF receptors family which are essential mediators of cell proliferation and differentiation. Overexpression of these receptors positively correlates with transphosphorylation and increased tumour growth rates [17]. A recombinant DNA construct of αHER2 IgG was specially engineered to contain LPETG sortase-tag at the C-termini of the two heavy chains ($\alpha HER2_{LPETG}$ IgG) to enable site-specific SrtA mediated azide bioconjugation (SMAB) and subsequent SPAAC driven attachment to modified NSNE-BCN surface. Hereby we introduce a facile protocol for the development of αHER2-functionalised doxorubicin-loaded NSNE as an innovative nanosized cargosystem with the potential to be used as a universal cancer therapeutic.

2. Results and discussion

Flow through ultrasonication provided a simple, fast, versatile and green pathway for synthesizing the novel protein-shelled nanocarrier system; nisin-shelled nanoemulsion (NSNE). NSNE preparation started by emulsifying soybean oil (10 w%) in an aqueous buffered solution containing nisin (1 mg/mL) and non-ionic surfactants to reduce the interfacial tension and improve the colloidal stability of the emulsion [18]. Next, flow through ultrasonication (20 kHz) horn shown in Fig. 1**A**, was used to create high shear stress by acoustic cavitation and rupture the o/w emulsion into a monodispersed nanoemulsion.

The obtained nanovesicles have a size distribution of 100 ± 20 nm as measured by dynamic light scattering and a zeta potential value of −50 mV. This negative surface charge can be explained by the organization of nisin at NSNE interface; whereby the acidic amino acids (aminobutyric acid) are twice exposed at the surface in relation to the basic amino acids, located further down the peptide chain, and facing the lipophilic core.

HPLC and Mass spectroscopy analyses were performed to prove nisin is present at the o/w interface and formed a shell coating the oil nanodroplets. HPLC chromatograms of the formulation before ultrasonication (Fig. 1**B**) show nisin peaks at retention time of 16.5 and 17.5 min. However, the analysis of the solution after sonication and separation of NSNE indicated the disappearance of the peak. This suggests that all nisin molecules are deposited at the oil–water interface. Mass spectrometry analysis also confirmed the disappearance of the nisin peaks in the solution after the ultrasonic emulsification and separation of NSNE. Overall these results indicate that nisin is incorporated into the nanodroplets (NSNE), most probably, in the form of a shell due to its high surface activity. To further explore the antibacterial activity of nisin in NSNE, a nisin killing assay using *Staphylococcus aureus* ATCC-29213 was performed. The results of this dose-dependent study, shown in Fig. 1**C**, demonstrated the enhanced bactericidal potency for the NSNE over pure nisin. This result may be explained by the orientation of nisin at the nanoemulsion interface; whereby the lanthione rings A and B in nisin structure responsible for antibacterial recognition and binding [19] are well maintained and exposed on the surface of prepared NSNE. This, in addition to the possible synergistic bactericidal effect of other components incorporated in NSNE including surfactants.

To investigate the anticancer application of the developed nanovesicles, NSNE was post-loaded with the model chemotherapeutic drug, Doxorubicin, which can easily be loaded into the oil core of NNE through hydrophobic interactions [20]. Drug loading assessment showed that more than 65 % (0.045 mg/mL) of Doxorubicin was loaded into the $NSNE_{DOX}$ formulation (Nisin 1 mg/mL, Soybean 10 %). After loading, $NSNE_{DOX}$ nanovesicles increased in size from 100 ± 20 nm to 150 ± 20 nm in addition to becoming red in color (Fig. 1**D),** and zeta potential decreased from −50 mV to −3 mV (Fig. 1**E**). This physicochemical change can be attributed to the successful loading of the positively charged red colored doxorubicin (pKa = 8.2), not only in the oily core but also within the protein shell of the nanoemulsion compared to the unloaded NSNE. [21–22] Physicochemical characterization also highlighted the colloidal stability of $NSNE_{DOX}$ formulation over a period of 6 months and when spin-washed via centrifugation; manifested by only the minor change to their physicochemical characteristics (Fig. 1**E**).

The empty NSNE or drug loaded $NSNE_{DOX}$ provided a template for decorating the nanoparticle surface with a cancer targeting ligand; using a 'bio-click' approach. Initially, the amine groups available in the nisin shell were incubated with an amine reactive bifunctional linker (NHS-PEGx-BCN), to create structural motifs for SPAAC reaction on the nanocarriers surface (NSNE-BCN). The washed SPAAC reactive nanoemulsion was then mixed with a SFC probe at physiological conditions to verify the surface modification (Fig. 2**A**). A strong blue fluorescence was emitted after click activation of the SFC probe upon binding to the NSNE-BCN shell as confirmed by the fluorescence imaging **(**Fig. 2**A insert)**. This suggests that NSNE surface was successfully tethered with BCN click handles (NSNE-BCN) and made SPAAC reactive.

The SFC probe click reaction with NSNE-BCN at 37 °C was monitored by time-dependent fluorescence for at least 2 h as shown in Fig. 2**B**. Interestingly, the results showed a significant effect of the linker chain length on this reaction whereby stronger blue fluorescence was emitted ($p < 0.0001$) when the SFC probe was clicked to $NSNE\text{-}PEG_8BCN$ in comparison to the PEG_{12} linker. This might be explained by possible coiling of the longer linker chain (PEG_{12}) rendering the BCN group on

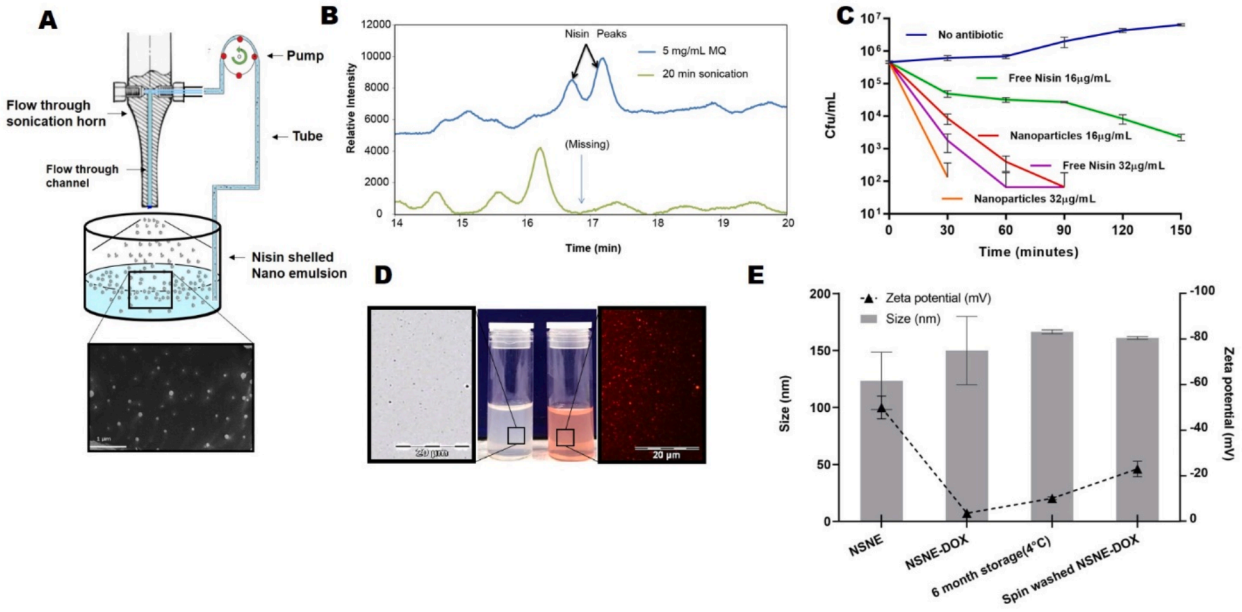

Fig. 1. Nisin-shelled nanoemulsion formulation using Flow-through Ultrasonication and characterization. (A) Schematic illustration for the Flow-through ultrasonicator machine and SEM image of the produced nanovesicles; scale 1 μm (B) HPLC chromatogram showing the presence and absence of nisin related peaks after nanovesicle formation (C) Bactericidal assay for nisin and NSNE when used in concentrations (16, 32 μg/mL) (D) Microscopical image of NSNE (translucent) and Doxorubicin loaded $NSNE_{DOX}$ (red) nanovesicles (E) Column chart displaying the physico-chemical properties (size and zeta-potential) of prepared NSNE, after Doxorubicin loading, after 6 month storage and after spin washing. Data represent means ± standard error of the mean based on at least 3 independent biological replicates.

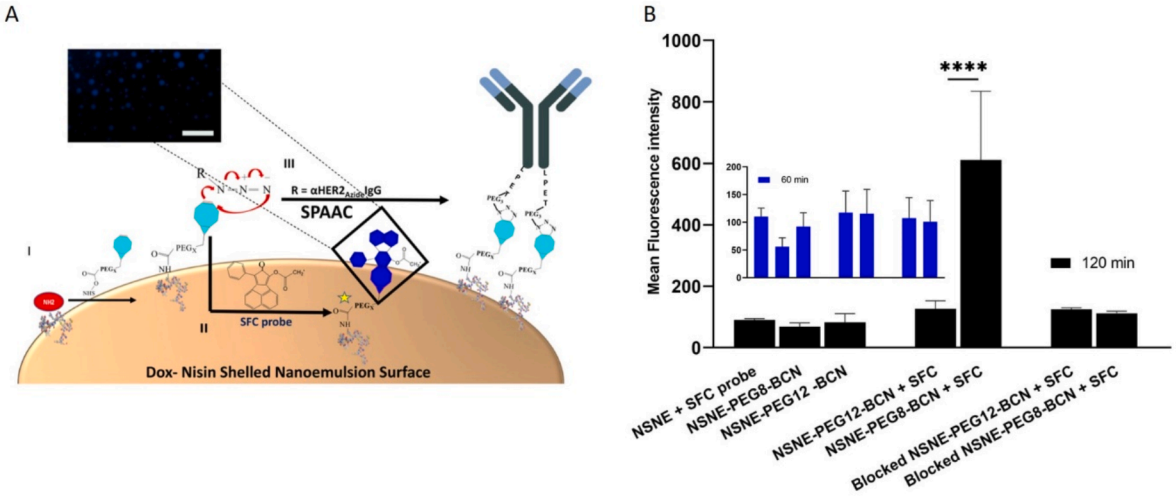

Fig. 2. Schematic illustration for creating a SPAAC-reactive surface on NSNE and validation using a click-activated smart florescent (SFC) probe. (I) Coupling of bifunctional linker (NHS-PEGx-BCN) to the amino groups in the surfaced lysine residues on the nisin shell. (II) A smart probe which emits florescence only when click activated (SFC), can bind to the attached BCN groups on NSNE surface and switch on the florescence as imaged using florescence microscopy (insert); Scale 10 μm. (III) Strain promoted alkyne azide cycloaddition (SPAAC) of an azide-bearing targeting antibody with BCN-functionalized NSNE. (B) Flow cytometry analysis of SFC probe click reaction to NSNE and NSNE-BCN (2 different chain lengths PEG_8-BCN and PEG_{12}-BCN) after 60 and 120 min compared with a pre-blocking treatment of nanovesicles. Data represent means ± standard error of the mean based on 3 independent replicates (two-way ANOVA using Tukey's multiple comparison test, ****$p < 0.0001$).

the nanoparticle surface not accessible for the click reaction and SFC attachment. As a control experiment, pre-treatment of NSNE-BCN with a blocker (an equimolar concentration of NaN_3) showed no detectable null signal confirming the specific reactivity of SFC probe to the BCN moieties on NSNE-BCN surface.

Using recombinant DNA technology, a unique pentapeptide LPETG motif was recombinantly engineered onto the targeting antibody ($\alpha HER2_{LPETG}$ IgG), to be recognized by SrtA, and was placed at the C-terminus of both heavy chains to preserve its receptor binding affinity. Accordingly, SrtA and $\alpha HER2_{LPETG}$ IgG were cloned, expressed, and purified as per methods described then quantified and identified using SDS PAGE gel as displayed in Fig. 3**B**. Biologically, SrtA normally catalyzes the attachment of a nucleophilic polyglycine moiety by cleaving between the threonine and glycine residues. In this research work SrtA mediated the bioconjugation of a G-PEG_3-Azide linker to both the C-termini of the targeting antibody ($\alpha HER2_{Azide}$ IgG) as schematically illustrated in Fig. 3**A.** A commercial αHER2 IgG (bearing no LPETG sequence) was used as a negative control to exclude unspecific reaction.

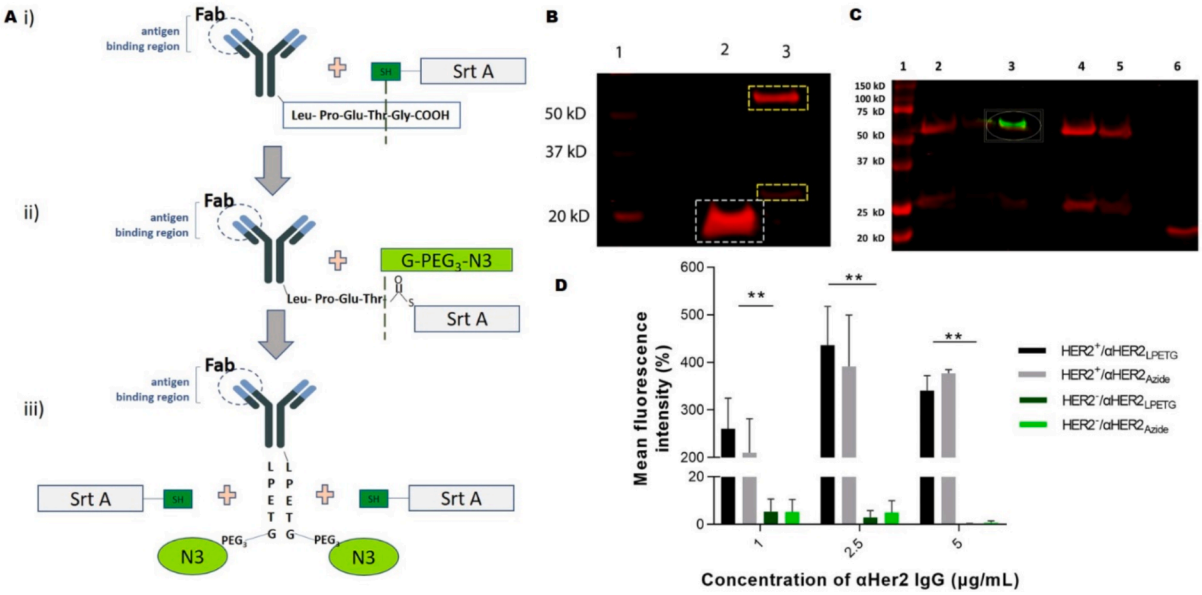

Fig. 3. SMAB and verification using SDS-PAGE gel electrophoresis. (A) Schematic illustration for the steps involved in the SrtA mediated bioconjugation of an azide group (SMAB) to the targeting antibody at genetically encoded LPETG tag. I) SrtA recognizes LPETG motif and cleaves between threonine and glycine to produce a thio-acyl intermediate. II)The exposed thioacyl group is then attacked by a nucleophilic poly-glycine component such as G-PEG3-Azide used in this study. III) The final product thus yields a click reactive azide-bearing antibody ($\alpha HER2_{Azide}$ IgG) and free SrTA. (B) Comassie stained SDS PAGE gel of successful cloned, expressed and purified SrtA enzyme (lane 2) and $\alpha HER2_{LPETG}$ IgG (lane 3). (C) The success of SMAB on $\alpha HER2_{LPETG}$ IgG was verified when 20 ug protein samples were incubated with BCN-Dylight 800 (a click reactive fluorophore) then run on 12 % SDS -PAGE gel and Comassie stained. Using Odyssey CLx® -imaging system the gel was scanned at 700/800 nm NIR wavelength showing: molecular weight protein standard markers (lane 1), lanes 2 and 3 for $\alpha HER2_{LPETG}$ IgG before and after SMAB, respectively, while lanes 4 and 5 corresponding to commercial αHER2 IgG before and after SMAB. (D) Binding of $\alpha HER2_{LPETG}$ in comparison to the $\alpha HER2_{Azide}$ on HER^+ and HER^- cell lines which shown no difference in the affinity to the target after sortase A modification and also no uptake on the non-antigen expressing cell line. Data represent means ± standard error o the mean based on 3 independent biological replicates (two-way ANOVA using Tukey's multiple comparison test, **p < 0.01).

Successful production of a click reactive antibody ($\alpha HER2_{Azide}$ IgG) via SMAB approach, was verified using a click reactive near-infrared/ green fluorescent dye (BCN-DL800) then run on SDS-PAGE gel and visualized using NIR-fluorescence imaging in the 800 nm channel wavelength. A strong green fluorescent band was detected for $\alpha HER2_{Azide}$ IgG heavy chain (lane3 Fig. 3**C**) in comparison to the commercial αHER2-IgG sample which showed no green fluorescence (lane 5). This observation confirmed the site-specific SMAB reaction at the C-terminus of both heavy chains of $\alpha HER2_{Azide}$ IgG (greater than50 kDa) and the availability of its azide functionalization for SPAAC reactions.

The receptor binding efficiency of ($\alpha HER2_{Azide}$ IgG) after SMAB was evaluated using flow cytometry. The results displayed in Fig. 3D demonstrate the comparable tumour cell binding efficiency of targeting ligand before and after SMAB ($\alpha HER2_{LPETG}$ IgG, $\alpha HER2_{Azide}$ IgG) at all three concentrations. Furthermore, statistically significant binding to HER2 expressing in comparison to HER2 non-expressing cells ($p < 0.0001$) was observed and demonstrated the specificity of α-HER2 IgG as a tumour targeting ligand. In the meantime, 2.5 ug/mL concentration was chosen for upcoming experiments due to the highest binding capacity.

SPAAC click reaction drove the final step for targeted particle assembly. A spontaneous bioorthogonal and site-specific covalent bonding between SPAAC-reactive azide-bearing αHER2 IgG with complementary SPAAC-reactive BCN-functionalized $NSNE_{DOX}$ led to the generation of novel cancer targeting nanovesicles of doxorubicin-loaded nisin shelled nanoemulsion surface-decorated with αHER2 IgG ($NSNE_{DOX}$-αHER2 IgG). To investigate the final amount of conjugated antibody to the nanovesicles, the flow through post spin filter wash was analysed. Furthermore, specificity of the click conjugation vs unspecific adsorption was investigated by three hours pre-incubation of NSNE-BCN with a complimentary click reactive compound before incubation with $\alpha HER2_{Azide}$ IgG. The analysis of the flow through post spin filter wash indicated that the majority of the antibody (up to 85 ± 2 %) was site-specifically clicked to the NSNE-BCN while only 15 ± 2 % of the antibody was found to be physically adsorbed.

In addition, the nanosystem characteristics as particles size and Polydispersity index after conjugation was characterized using dynamic light scattering (DLS). The results as displayed in Fig. 4 **A**, showed no significant changes in nanosystem ($NSNE_{DOX}$-αHER2) particle size and homogeneity before and after antibody conjugation.

Importantly, *in vitro* plasma stability assay provides helpful insight into how blood components affect the size and aggregation behaviour of drug delivery vehicles once injected into blood plasma [23]. The interactions between NSNE particles and blood plasma did not lead to multicomponent aggregation of particles or plasma components as assessed by DLS. There was also no indication of particle degradation. However, a slight increase in particle size over time was observed, without reaching significant differences (Fig. 4**B**) [24]. These results provide an indication that the particles are stable in plasma and that the nisin protein coating plays an important role by decreasing multicomponent aggregation in plasma.

Finally, the anti-cancer activity of tumour-targeted $NSNE_{DOX}$-αHER2 IgG were explored. The cancer targeting efficiency of assembled $NSNE_{DOX}$-αHER2 IgG to HER2-expressing cancer cells was validated using flow cytometry. As shown in Fig. 4**C**, we observed significant increase of $NSNE_{DOX}$-αHER2-IgG association to $HER2^+$ cells in comparison to $HER2^-$ cells ($p < 0.01$). These results indicate that αHER2 IgG, model targeting ligand, was able to attach site- specifically to the surface of $NSNE_{DOX}$-BCN nanovesicles and retain its tumour targeting efficiency. Such cancer specific targeting of $NSNE_{DOX}$-αHER2 IgG was further confirmed by pre-blocking the antigen binding site on the cancer cells with commercially available HER2 mAb before adding $NSNE_{DOX}$-αHER2 IgG; a significant reduction in receptor binding was observed ($p < 0.01$).

Additionally, a WST-1 assay, a technique for colorimetric evaluation

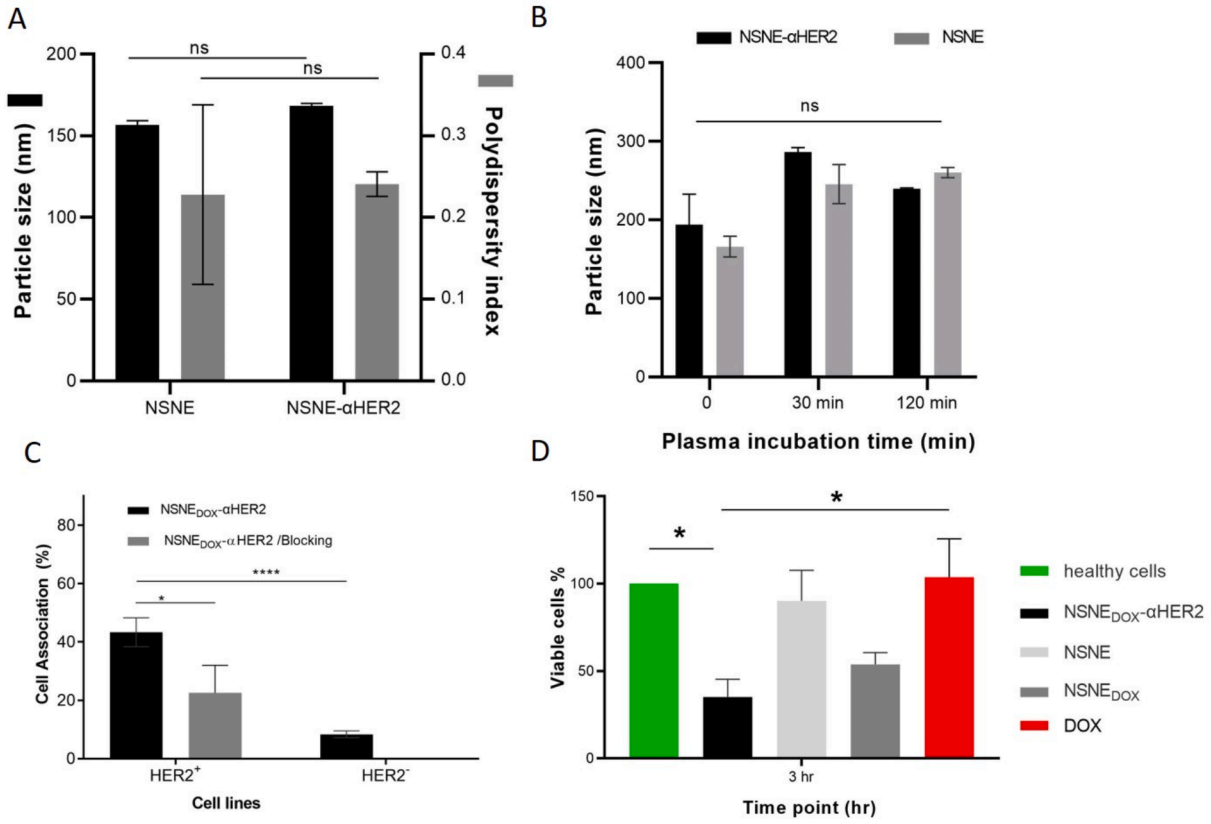

Fig. 4. Targeted nanovesicles characterization: (A) Particle size (ps) and polydispersity (pdi) analysis of the nanosystem before (NSNE) and after antibody conjugation (NSNE-αHER2) using dynamic light scattering. (B) In vitro plasma stability by incubation of targeted NSNE-αHER2 IgG in plasma for 0, 30 and 120 min. (C) Tumour cell association efficiency of targeted NSNE$_{DOX}$-αHER2 IgG to HER2$^+$and HER2$^-$ cancer cell lines compared to a receptor pre-blocking with commercially available HER2 mAb to determine specificity (D) Variability assay by incubating HER2$^+$ cancer cells 3hr with the targeted NSNE$_{DOX}$-αHER2 IgG in comparison to Doxorubicin, NSNE, NSNE$_{DOX}$. Data represent means ± standard error of the mean based on 3 independent biological replicates (two-way ANOVA using Tukey's multiple comparison test with *p < 0.05 or greater as significant; *t*-test within two sample groups, ns = not significant).

of cell proliferation assay, was used to quantitatively assess the degree of HER2$^+$ cancer cell death after application of NSNE$_{DOX}$-αHER2 IgG and controls such as Doxorubicin, NSNE and nontargeted NSNE$_{DOX}$. The parameters of this assay were as followed 1 μg of Doxorubicin and incubated 3 h period. The results indicated a significant decrease in cancer cell viability upon treatment with targeted NSNE$_{DOX}$-αHER2 IgG (1 μg Doxorubicin) in comparison to the free drug (Doxorubicin) (Fig. 4**D**). This enhanced cytotoxic effect indicates a faster and higher potency of NSNE$_{DOX}$-αHER2 IgG compared to its controls and shown in literature [24–25]. Future studies will be beneficial to observe the cellular uptake of this novel nanosystem and its biodistribution and tumour accumulation *in vivo*.

3. Conclusion

The outstanding benefits of nisin, as a polypeptide, were the basis for developing a novel nanovesicle, Nisin-shelled nanoemulsion (NSNE), which when loaded with a special payload and decorated with a targeting ligand become a universal nanosized-platform for therapeutic/ diagnostic applications. The results in this research work revealed that flow-through ultrasonication proved to be the method of choice to produce spherical and uniformly dispersed nanovesicles of NSNE with long term stability, low toxicity and, even more, able to accommodate a high concentration of anticancer drugs and augment their cytotoxic effect. All components of the NSNE are biodegradable and biocompatible. A unique two phase (bio-click) approach, involving both SMAB/SPAAC reactions, was efficient in the site-specific attachment of cancer targeting ligand (αHER2$_{LPETG}$ IgG) on nisin shelled nanovesicles. Finally, biological assays proved that nisin was assembled at the water–oil interface in a way where the antibacterial binding region (AB ring fragment) in nisin structure and the lysine residue 12 are directed outwards in the aqueous phase and are exposed for surface reactions. Therefore, as more interest is currently drawn for bacterial infections in cancer patients, the combined bactericidal/ cytotoxic effect of NSNE when loaded with a cytotoxic drug paves the way for a dual therapy platform for bacterial infections in cancer patients.

4. Experimental Methods

4.1. Flow through ultrasonication method for the preparation of Nisin-shelled nanoemulsion

The general scheme for preparing NSNE involves a two-step emulsification method at room temperature. Initially, coarse o/w emulsion was prepared by magnetically stirring 10 % soybean oil (dispersed phase) in 10 mM sodium phosphate buffer containing 1 mg/mL nisin (continuous aqueous phase) and 5 w% of non-ionic surfactant (50 % Tween 80 and 50 % Span 80). The whole mixture was left to stir for 15 min. and final pH of the solution was adjusted to 7.5. Secondly, the coarse emulsion was subjected to a 20 kHz flow through ultrasonication horn (1 cm tip with 3 mm hole size) for 4–6 min, operated at an ultrasonic power about 240 W and flow rate optimized to 175 mL/min. Samples were taken every 2 min. for physicochemical characterization; using optical microscopy, dynamic light scattering and HPLC. Prepared nanoemulsion (NSNE) was dialyzed overnight and stored in fridge for upcoming experiments. Stability of the nanoemulsion was evaluated after 6 months storage in the fridge and when subjected to spin washing in Amicon® Ultra 0.5 mL 100 K Centrifugal Filters at 14,000 rpm for 5

min.

4.2. Physicochemical characterization

The presence of nisin in nanoemulsion was tracked by measuring the change in the nisin concentration using a RP-HPLC (SHIMADZU controller SCL-10AVP, oven CTO-10ASVP, pump LC-10ATVP, auto injector SIL-10ADVP, diode array detector APDM10AVP) with eluents A (Water: Acetonitrile: Trifluoro acetic acid 900:100:1) and B (Water: Acetonitrile: Tri fluoro acetic acid 100:900:1). Before analysis, samples were filtered using 0.45 μm syringe filters. A C18 column (Jupiter 5 μm, 300 A0, 250 × 4.6 mm) was used and the flow rate was 0.8 mL/min at room temperature. Malvern Zetasizer (Nano ZS) was used for particle size and surface charge analysis before and after antibody conjugation. Freshly prepared samples of nanoemulsions were diluted 10 times with deionized water and analysed under the 'protein size analysis' option (particle refractive index: 1.45, particle absorption 0.001, viscosity of water 0.8872 cP, refractive index of water 1.33, measurement angle: 173° backscatter). The morphologies of the samples were observed using a high- resolution field emission scanning electron microscope (Quanta 200 FEI) without sputter coating pre-treatment.

4.3. Nisin killing assay

Staphylococcus aureus strain ATCC 29213 was grown on Heart Infusion agar (Oxoid) at 37 °C for 16 h. Plate grown bacteria were harvested into Cation-Adjusted Mueller (CAMH) broth (Thermo Scientific), equalized to an optical density at 600 nm (OD600) = 1.0, and diluted to 1x106 CFU/mL. 50 μL of each suspension was added to wells of a 96 well plate in triplicate. The killing assay was started by addition of 50 μL free nisin or nisin nanoparticles in CAMH broth to a final concentration of either 16 or 32 μg/mL. 96 well plates were incubated at 37 °C and samples were taken at 30, 60, 90, 120 and 150 min. 10-fold serial dilutions were performed in CAMH broth, 5 μL of each dilution was plated onto the agar and plates were incubated at 37 °C for 16 h. Bactericidal activity was assessed.

4.4. Doxorubicin loading

Nisin o/w nanoemulsion was loaded with a model chemotherapeutic drug; Doxorubicin. Initially, ultracentrifugation (at 100,000*g* at 4 °C for 30 min) separated NSNE in the top layer which was collected and diluted to 1 mg/mL of nanoemulsion in aqueous solution. Afterwards, Doxorubicin (0.07 mg/mL) was incubated with NSNE overnight with gentle shaking then dialyzed overnight to get rid of unloaded doxorubicin. Doxorubicin, with inherent florescence at 600 nm, when loaded in NSNE was visualized using florescence microscopy, measured quantitively using florescence spectroscopy and characterized using Dynamic light scattering. Entrapment efficiency percentage of $NSNE_{DOX}$ was calculated according to equation: $[DOX_{total\ (g)} - DOX_{free\ (g)} / DOX_{total\ (g)}] \times 100$.

4.5. SPAAC reactive

An amine-reactive bifunctional linker (NHS-PEGx-BCN) was incubated with NSNE (1 mg/mL) in excess for 3 h at 4 °C on gentle rotation. The cross-linker chain lengths studied herein were two (PEG_8 and PEG_{12}). Surface modified nanovesicles NSNE-BCN were spin-washed 3 times in PBS, to remove any unreacted NHS-PEG4-BCN using Amicon® Ultra Centrifugal Filter at 14000xg for 5 min. Note only unloaded NSNE was used for assessment of this surface modification as the nisin shell was considered identical in both NSNE and $NSNE_{DOX}$.

4.6. Verification of NSNE-BCN surface modification

As per method described by Ji et al. [10] nanoemulsion samples were incubated with SFC in a 1:10 M ratio of probe: BCN-NSNE, then spin-washed using centrifugal filters. The parameters of this experiment were optimized; including reaction time (1 h and 2 h) and linker chain length (PEG8 and PEG 12). A control experiment was performed where a pre-treatment of NSNE-BCN with a blocker (an equimolar conc. of NaN3) before incubation with SFC probe. The intensity of florescence emitted was detected using BD FACS Canto II Flow Cytometer and analysed using FlowJo software. Fluorescence microscope imaged the fluorescent nanodroplets in the DAPI channel.

4.7. Recombinant DNA constructs of SrtA and $\alpha HER2_{LPETG}$-IgG cloning, expression and purification

Recombinant DNA technology was essential in the production of the transpeptidase enzyme (SrtA) and the cancer targeting ligand ($\alpha HER2_{LPETG}$-IgG) whereby their DNA sequences were cloned into *E.coli* expression plasmids then separated using Plasmid Maxiprep System (Promega). Afterwards, expression plasmids of $\alpha HER2_{LPETG}$-IgG were transfected into mammalian HEK293 cells while SrtA was transfected into bacterial E. coli. Expressed proteins were purified using FPLC chromatography based on nickel affinity and size exclusion using Ni-NTA Superflow columns. BCA assays were performed for colorimetric quantification of protein sample concentrations while SDS-PAGE was completed to evaluate the purity of protein samples, and gels were produced fresh.

4.8. SortaseA-mediated azide bioconjugation (SMAB) to $\alpha HER2_{LPETG}$-IgG

An LPETG recognition motif was genetically encoded in the construct of the targeting ligand ($\alpha HER2_{LPETG}$-IgG) for SrtA to site-specifically cleave and conjugate a click reactive azide moiety (SMAB). The expressed and purified $\alpha HER2_{LPETG}$-IgG was mixed with SrtA and the bifunctional G-PEG4-Azide linker in a 1:6:3 M ratio, respectively. The reaction proceeded for 5 h at 37 °C in the presence of sortase reaction buffer (50 mM Tris, 150 mM NaCl, 0.5 mM $CaCl_2$ pH 8.0). Finally, purification of $\alpha HER2_{Azide}$-IgG was completed using a Nuvia™ IMAC Resin (Biorad ltd) as described by manufacturer. The flow-through containing $\alpha HER2_{Azide}$-IgG only was collected and dialyzed against PBS overnight at 4 °C, as SrtA would be removed from the reaction product due to the his-tag, in its construct, affinity to the resin. BCA assays were performed for colorimetric quantification of SMAB-modified ligand ($\alpha HER2_{Azide}$-IgG) concentrations.

4.9. Verification of successful SMAB-modification to $\alpha HER2_{Azide}$-IgG

Samples of $\alpha HER2_{LPETG}$-IgG and commercial αHER2-IgG (not bearing LPETG sequence) before and after SMAB were incubated with a near infrared fluorescent click reactive dye (BCN-Dylight 800) then run on freshly prepared SDS-PAGE gel, Coomassie stained and scanned 700/800 nm NIR wavelength using Odyssey CLx® -imaging system.

4.10. SPAAC-mediated targeted particle assembly ($NSNE_{DOX}$-αHER2 IgG)

SPAAC was the driving force for targeted nanovesicle assembly. SPAAC reactive Doxorubicinloaded nanoemulsion ($NSNE_{DOX}$-BCN) was mixed with SPAAC reactive azide- bearing $\alpha HER2_{Azide}$-IgG and incubated for 3 h under gentle rotation at room temperature. The reaction mixture was spin-washed and stored at 4 °C for further experimentation.

For site specific antibody conjugation quantification, the through flow after wash spin was analysed using BCA assay as $Wt_{antibody\ unconjugated}$). Percentage of antibody conjugation was calculated according to following equation:

$$\text{Percentage of antibody conjugated}: 100\,\% - .\left(\frac{\text{Wt antibody unconjugated}}{\text{Wt total antibody}} \times 100\right)$$

Specificity was determined by pre-blocking of the binding site via azide-click groups in a threefold molar access for 3 h. The blocked nanoparticles were spin washed then incubated with the azide- labelled $\alpha HER2_{Azide}$-IgG and left for another 3 h at room temperature. The system was then spin washed and analysed for remaining unconjugated antibody using BCA assay. Percentage of unspecific and specific antibody conjugation was calculated according to following equation:

$$\text{Percentage of unspecific antibody conjugation}: 100\,\% - \left(\frac{\text{Wt antibody unconjugated}}{\text{Wt total antibody}} \times 100\right)$$

Particle diameter, size distribution and morphology were monitored after antibody conjugation using dynamic light scattering and Scanning Electron Microscopy.

4.11. Tumour cell receptor binding efficiency

Tumour cell lines expressing and non-expressing HER2 receptors were seeded overnight. 1.5×10^4 cells/well were collected and incubated with various treatment including targeting ligand αHER2-IgG before and after SMAB in 3 different dilutions (1, 2.5 and 5 μg/mL) or the targeted nanovesicles $NSNE_{DOX}$-αHER2-IgG aliquots containing 1ug Doxorubicin. A blocking treatment of the two cell lines with commercial analog of αHER2-IgG was investigated as a pretreatment before incubating with $NSNE_{DOX}$-αHER2-IgG. Receptor binding efficiency was detected using antiHuman IgG-488 florescent mAb via flow cytometry.

4.12. WST-1 cytotoxic assay

HER2 expressing cancer cells were seeded in $DMEM^+$ media at 1.5×10^4 cells/well in a flat-bottom Corning® Costar® 96-well microplate, and grown for 24 h until an 80 % confluent cell layer was formed. Original $DMEM^+$ media was removed, and the various treatments in fresh media were added to cells up to 100 μL/well, 3 h time points, incubated the microplate at 37 °C then 10 μL/well of the reaction solution Cell Proliferation Reagent WST-1 (Merck) was then added and again incubated at 37 °C for a further 90 min. The spectrophotometrical absorbance values of samples were then measured at 450 nm using the FLUOstar OPTIMA Microplate Spectrophotometer. All values were then calculated as percentages relative to wells of DMEM + media while viable and untreated cells at each time point was used to normalize the maximum cell viability to 100 % and hence measure the *in vitro* cytotoxicity of treatments.

4.13. In vitro plasma stability

The *in vitro* plasma stability of the nanosystem was studied in human plasma. Initially, blood was withdrawn from healthy volunteers (0.5 % volume of 3.2 % w/v sodium citrate added as an anticoagulant) according to ethics approval number CF07/0141–2007/0025). The whole blood was then centrifuged at 1000 rpm for 10 min and the blood plasma was separated from the blood cells. Plasma stability testing was initiated by the addition of 100 uL of particle solution (NSNE, $NSNE_{DOX}$-αHER2-IgG) to 1 mL of preheated plasma solution. The particles were incubated in the blood plasma continuously for 120 min in a shaking water bath at 37 °C. Samples were taken at 0, 30 and 120 min, diluted twofold using preheated PBS for ideal DLS analysis using Malvern Zetasizer (Nano ZS). Dynamic light scattering (DLS) was used to monitor the change in particle characteristics (size and PDI). The values represent the mean of three independent experiments.

4.14. Statistical analysis:

One-way analysis of variance was used to determine statistical significance. The results are expressed as means ± the standard error of the mean. *P*-values < 0.05 were considered statistically significant. All statistical analyses were performed using Graphpad prism V9.4.1.

Declaration of Competing Interest

The authors declare that they have no known competing financial interests or personal relationships that could have appeared to influence the work reported in this paper.

Data availability

Data will be made available on request.

Acknowledgments

The authors would like to thank Shweta Jagdale for technical assistance. This work is supported by the National Health and Medical Research Council of Australia (Career Development Fellowship GNT1140465 to K.A., Senior Research Fellowship to C.E.H. GNT1154270). The authors also wish to thank AMREP Flow Cytometry Core Facility (Eva Orlowski-Oliver and Dr Magdaline Costa) and Binghe Wang (Department of Chemistry and Center for Diagnostics and Therapeutics, Georgia State University, Atlanta, Georgia 30303 United States) for kindly providing the *click-activated smart florescent (SFC) probe.*

References

[1] B. Choi, H. Kim, H. Choi, S. Kang, Protein cage nanoparticles as delivery nanoplatforms, Adv. Exp. Med. Biol. 1064 (2018) 27–43.
[2] A. Franzetti, P. Di Gennaro, A. Bevilacqua, M. Papacchini, G. Bestetti, Environmental features of two commercial surfactants widely used in soil remediation, Chemosphere 62 (9) (2006) 1474–1480.
[3] L. Bao, L. Bian, M. Zhao, J. Lei, J. Wang, Synthesis and self-assembly behavior of a biodegradable and sustainable soybean oil-based copolymer nanomicelle, Nanoscale Res. Lett. 9 (1) (2014) 391.
[4] K. DeFrates, T. Markiewicz, P. Gallo, A. Rack, A. Weyhmiller, B. Jarmusik, X. Hu, Protein polymer-based nanoparticles: fabrication and medical applications, Int. J. Mol. Sci. 19 (6) (2018).
[5] S.K. Bhangu, A. Baral, H. Zhu, M. Ashokkumar, F. Cavalieri, Sound methods for the synthesis of nanoparticles from biological molecules, Nanoscale Adv. 3 (17) (2021) 4907–4917.
[6] M. Zhou, F. Cavalieri, F. Caruso, M. Ashokkumar, Confinement of acoustic cavitation for the synthesis of protein-shelled nanobubbles for diagnostics and nucleic acid delivery, ACS Macro Lett. 1 (7) (2012) 853–856.
[7] A. Gharsallaoui, N. Oulahal, C. Joly, P. Degraeve, Nisin as a food preservative: Part 1: physicochemical properties, antimicrobial activity, and main uses, Crit. Rev. Food Sci. Nutr. 56 (8) (2016) 1262–1274.
[8] N.E. Joo, K. Ritchie, P. Kamarajan, D. Miao, Y.L. Kapila, Nisin, an apoptogenic bacteriocin and food preservative, attenuates HNSCC tumorigenesis via CHAC1, Cancer Med. 1 (3) (2012) 295–305.
[9] A.N. Marcos, U. P., K. Uemura, C. Takahashi, I. Kobayashi, P. Romano, M. Nakajima, J. Food Sci Eng. 6 (63) (2016).
[10] X. Ji, K. Ji, V. Chittavong, R.E. Aghoghovbia, M. Zhu, B. Wang, Click and fluoresce: a bioorthogonally activated smart probe for wash-free fluorescent labeling of biomolecules, J. Organ. Chem. 82 (3) (2017) 1471–1476.
[11] C.S. McKay, M.G. Finn, Click chemistry in complex mixtures: bioorthogonal bioconjugation, Chem. Biol. 21 (9) (2014) 1075–1101.
[12] E. Lallana, E. Fernandez-Megia, R. Riguera, Surpassing the use of copper in the click functionalization of polymeric nanostructures: a strain-promoted approach, J. Am. Chem. Soc. 131 (16) (2009) 5748–5750.
[13] K. Alt, B.M. Paterson, E. Westein, S.E. Rudd, S.S. Poniger, S. Jagdale, K. Ardipradja, T.U. Connell, G.Y. Krippner, A.K. Nair, X. Wang, H.J. Tochon-Danguy, P. S. Donnelly, K. Peter, C.E. Hagemeyer, A versatile approach for the site-specific modification of recombinant antibodies using a combination of enzyme-mediated bioconjugation and click chemistry, Angew. Chem. Int. Ed. Engl. 54 (26) (2015) 7515–7519.
[14] C.E. Hagemeyer, K. Alt, A.P. Johnston, G.K. Such, H.T. Ta, M.K. Leung, S. Prabhu, X. Wang, F. Caruso, K. Peter, Particle generation, functionalization and sortase A-mediated modification with targeting of single-chain antibodies for diagnostic and therapeutic use, Nat. Protoc. 10 (1) (2015) 90–105.

[15] Hashad, R. A.; Lange, J. L.; Tan, N. C. W.; Alt, K.; Hagemeyer, C. E., Engineering Antibodies with C-Terminal Sortase-Mediated Modification for Targeted Nanomedicine. In *Bioconjugation: Methods and Protocols*, Massa, S.; Devoogdt, N., Eds. Springer New York: New York, NY, 2019; pp 67-80.
[16] S.K. Mazmanian, G. Liu, H. Ton-That, O. Schneewind, Staphylococcus aureus sortase, an enzyme that anchors surface proteins to the cell wall, Science 285 (5428) (1999) 760–763.
[17] N. Iqbal, N. Iqbal, Human epidermal growth factor receptor 2 (HER2) in cancers: overexpression and therapeutic implications, Mol. Biol. Int. 2014 (2014), 852748.
[18] D.J. McClements, Emulsion design to improve the delivery of functional lipophilic components, Annu. Rev. Food Sci. Technol. 1 (2010) 241–269.
[19] I. Panina, N. Krylov, D. Nolde, R. Efremov, A. Chugunov, Environmental and dynamic effects explain how nisin captures membrane-bound lipid II, Sci. Rep. 10 (1) (2020) 8821.
[20] Y.Y. Diao, H.Y. Li, Y.H. Fu, M. Han, Y.L. Hu, H.L. Jiang, Y. Tsutsumi, Q.C. Wei, D. W. Chen, J.Q. Gao, Doxorubicin-loaded PEG-PCL copolymer micelles enhance cytotoxicity and intracellular accumulation of doxorubicin in adriamycin-resistant tumor cells, Int. J. Nanomed. 6 (2011) 1955–1962.
[21] N. Kaushal, Z.-S. Chen, S. Lin, Double-coated poly(butyl Cyanoacrylate) nanoparticles as a potential carrier for overcoming P-Gp- and BCRP-mediated multidrug resistance in cancer cells, Front. Nanotechnol. 3 (2021).
[22] X. Zhao, Q. Chen, W. Liu, Y. Li, H. Tang, X. Liu, X. Yang, Codelivery of doxorubicin and curcumin with lipid nanoparticles results in improved efficacy of chemotherapy in liver cancer, Int. J. Nanomed. 10 (2015) 257–270.
[23] M.S. Bannon, A. López Ruiz, K. Corrotea Reyes, M. Marquez, Z. Wallizadeh, M. Savarmand, C.A. LaPres, J. Lahann, K. McEnnis, Nanoparticle tracking analysis of polymer nanoparticles in blood plasma, Part. Part. Syst. Char. 38 (6) (2021) 2100016.
[24] B. Layek, T. Sadhukha, J. Panyam, S. Prabha, Nano-engineered mesenchymal stem cells increase therapeutic efficacy of anticancer drug through true active tumor targeting, Mol. Cancer Ther. 17 (6) (2018) 1196–1206.
[25] H. Huang, P. Li, C. Liu, H. Ma, H. Huang, Y. Lin, C. Wang, Y. Yang, pH-Responsive nanodrug encapsulated by tannic acid complex for controlled drug delivery, RSC Adv. 7 (5) (2017) 2829–2835.